ChemComm
Chemical Communications

Accepted Manuscript

This article can be cited before page numbers have been issued, to do this please use: J. Chang, H. Li and F. Li, *Chem. Commun.*, 2019, DOI: 10.1039/C9CC05022A.

ROYAL SOCIETY OF CHEMISTRY

rsc.li/chemcomm

View Article Online
DOI: 10.1039/C9CC05022A

COMMUNICATION

Diffusivity and Intercalation of Electroactive Dyes-Mediated Truly Ratiometric Homogeneous Electrochemical Strategy for Highly Sensitive Biosensing

Received 00th January 20xx,
Accepted 00th January 20xx

DOI: 10.1039/x0xx00000x

Jiafu Chang,[ab] Haiyin Li,[b]* and Feng Li[ab]*

A truly ratiometric homogeneous electrochemical biosensor has been developed for miRNA sensitive detection based on the unique diffusion/intercalation characters of electroactive dyes without the need to electrode modification or material preparation.

Ratiometric analysis permits self-calibration, decreases experimental and environmental interferences, and improves the diagnosis accuracy.[1, 2] Up to now, substantial efforts have been done to develop ratiometric biosensors, and to the best of our knowledge, the reported ratiometric biosensors focused mainly on fluorescence technique.[3-9] Undoubtedly, these proposed biosensors have secured the tremendous success in the cause of analyzing target analytes in biological matrixes. However, there are still some undeniable drawbacks associated with these biosensors that greatly impeded their widespread utilization in the biomedical field. Among them, the greatest obstacle is the difficult design and development of ratiometric biosensors with optimal sensing performance. Most of ratiometric biosensors are currently realized through the fluorescence resonance energy transfer (FRET) between the well-designed donors and acceptors,[4-6] but the fabrication process of which is both intricate and strict. Another strategy to achieve the ratiometric analysis is to introduce the signal materials with non-interfering excitation and emission wavelengths,[10] but which is bad for completing the detection in one single assay, and also needs a great deal of time and effort to design and prepare the signal materials.

Compared with ratiometric fluorescence biosensors, ratiometric electrochemical biosensors that employ the ratio change of dual current intensities under different potentials as signal output can be readily developed with the features of simpleness, rapidness, sensitivity, and low cost.[11] Furthermore, they can effectively avoid the interference of the colored substances that may be present in biological samples. These unique advantages make them as popular tools in the efficient analysis of miRNA,[12] protein,[13, 14] gene,[15] metal ions,[16] and so on.[17, 18] To realize the design and development of ratiometric electrochemical biosensor, immobilizing electroactive dyes labeled single-strand(ss)/double-strand(ds)/hairpin deoxyribonucleic acid (DNA) on electrode has become a subject of hot research interest. Unfortunately, the immobilization procedure is fussy, time-consuming, and laborious, and inappropriate immobilization methods may lead to false positive diagnosis result. More severely, the immobilization operation would make gigantic influence on the bioactivity of the recognizable probes because of the electrode's inherent hindered effect.[19, 20] A strategy to address these issues is to introduce immobilization–free (homogeneous) strategy into ratiometric electrochemical biosensors. However, according to our understanding, few efforts have been made on ratiometric homogeneous electrochemical (RHE) biosensors due to their superior difficulty in design except two relevant works reported by our group.[21,22] Among them, one was developed through the functionalized modification of the electrode, which needs strict experimental conditions to pledge the repeatability of the modified electrodes. Furthermore, the modified electrode can adsorb also other ssDNA that may exist in sensing system or biological matrixes, which would make significant influence on the diagnosis accuracy.[21] The other biosensor was proposed via a ssDNA-functionalized silica nanoparticle (SN), which requires the tedious synthetic steps, including the fabrication of SN, encapsulation of electroactive dye and functionalized modification of ssDNA on SN.[22] Besides, it is unstable due to the weak electrostatic interaction between ssDNA and SN, making bad to practical application. Moreover, their reactions happen not in the homogeneous solution.

To solve these issues and as a continuation of RHE biosensor, we proposed, herein, a novel RHE biosensor without the involvement of electrode modification or material preparation. The basis of this study for RHE biosensor development is the different diffusivity of electroactive dyes toward indium tin oxide (ITO) electrode under different existing forms. To illustrate the characteristic, different pulse voltammetry (DPV) responses of ferrocene-labeled ssDNA (Fc-ssDNA) and free methylene blue (MB) molecules were investigated under different conditions. As illustrated in Fig. 1A and B, the Fc-ssDNA was blocked from arriving at the ITO electrode because of the strong electrostatic repulsion between them, thus leading to a relatively weak DPV signal (23.51 nA). However, when Exonuclease I

[a] College of Chemistry, Chemical Engineering and Materials Science, Shandong Normal University, Jinan 250014, People's Republic of China
[b] College of Chemistry and Pharmaceutical Sciences, Qingdao Agricultural University, Qingdao, 266109, People's Republic of China. E-mail: lifeng@qau.edu.cn
Electronic Supplementary Information (ESI) available: [details of any supplementary information available should be included here]. See DOI: 10.1039/x0xx00000x

(Exo I) is present, the digestion of Fc-ssDNA by Exo I contributes to the appearance and growth in quantity of Fc-tagged mononucleotides (Fc-mNs), the diffusion of which toward ITO electrode was significantly enhanced due to their relatively small size and little negative charge, subsequently bringing about an obviously increased Fc signal (231.01 nA). Furthermore, from Fig. 1C and D, it can be clear seen that DNA molecules with different configurations (ssDNA, dsDNA, and G-quadruplex DNA) make different influence on DPV signal of MB. Free MB molecules in solution display a very high diffusivity toward ITO electrode, thus leading to a remarkably enhanced DPV current (243.15 nA). When ssDNA was added into the solution, the DPV current of MB was negligibly influenced. Contrarily, when dsDNA or G-quadruplex DNA was present, the DPV signal decreased significantly with the value of only 142.87 or 72.17 nA, respectively. It can be ascribed to the fact that MB molecules can effectively intercalate into dsDNA and G-quadruplex, and are trapped into the DNA chains, thus hampering the diffusion of MB toward ITO electrode because of the electrostatic repulsion between DNA molecules and negatively charged electrode.[23, 24] In addition, both Fc and MB have the non-interfering oxidation potentials located at 0.41 V and -0.23 V, respectively (Fig. S1). On the basis of the diffusion/intercalation characteristics of Fc and MB, we believe that it is feasible to develop RHE biosensor by using Fc-labeled DNA and free MB as the probes.

The principle of devising a RHE strategy for highly sensitive detection of miRNA-182 (used as the model target, and is closely relevant with the pathogenesis of gliomas, which is the most common primary brain tumour[25-27]) is illustrated in Scheme 1. The proposed system features two ingeniously cascaded signal amplification strategies by Exonuclease III (Exo III), which just needed three carefully designed DNA probes (Fc-H1, H2, and H3) and free MB molecules. When target miRNA-182 was absent in solution, Fc-H1, H2, and H3 maintain their hairpin configurations unchanged. As the weak diffusion of Fc-H1 toward ITO electrode significantly makes Fc tags away from electrode, the Fc-H1 affords a relatively low DPV signal. Meanwhile, small amount of MB

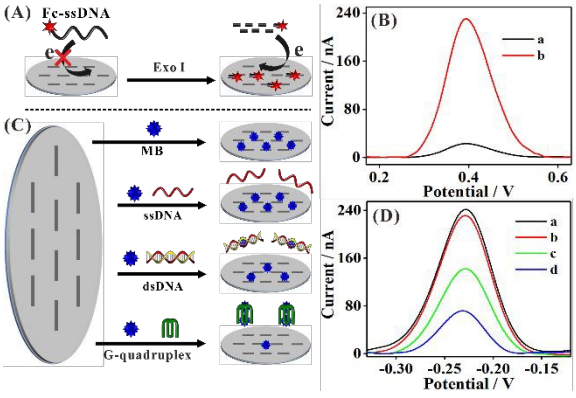

Fig. 1 (A) The diagram illustration of the affect of Exo I on the DPV response of Fc-ssDNA. (B) The DPV curves of Fc-ssDNA (1.0 μM) in the absence (a) and presence (b) of Exo I (0.2 U/μL). (C) The diagram illustration of the affect of ssDNA (P1), dsDNA (P1@P2), and G-quadruplex DNA (G1) on the DPV response of MB. (D) The DPV curves of MB under varied conditions: (a) free MB molecules; (b) MB + P1-ssDNA; (c) MB + P1@P2-dsDNA; (d) MB + G-quadruplex DNA. Experiments condition: [MB] = 2.0 μM; [P1] = 1.0 μM; [P2] = 1.0 μM; [G1] = 1.0 μM.

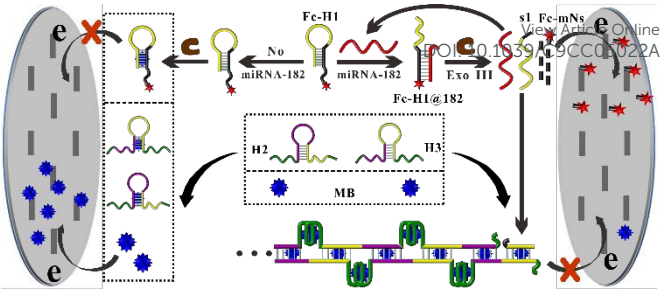

Scheme 1 The diagram illustration of the mechanism for RHE detection of miRNA based on the Exo III-assisted signal transduction/amplification reaction and the intrinsic diffusion/intercalation characters of electroactive dyes.

molecules are locked into the stems in Fc-H1, H2 and H3, while large numbers of MB molecules are free in the sensing system and enjoy high diffusion toward ITO electrode, which efficiently makes MB near to the electrode, guaranteeing a high current response of MB.

Whereas, when target miRNA-182 is introduced into the sensing system, the hybridization recognition of Fc-H1 by miRNA-182 impels the formation of Fc-H1@182 complexes. Then the Fc-H1@182 complexes were efficiently digested by Exo III, thus contributing to the release of ssDNA trigger s1 and the production of Fc-mNs, which significantly enhance the current response of Fc due to the increased diffusion to ITO electrode. The released s1 initiated the hybridization chain reaction (HCR) of H2 and H3 to form a long chain of dsDNA with single-strand overhang on the 3' and 5' ends, which brings them close to each other to form G-quadruplexes in the presence of K^+. Due to the stronger intercalation ability of MB into dsDNA and G-quadruplexes, larger amounts of MB molecules were trapped and prevented from moving to ITO electrode, affording an obviously declined DPV signal of MB. Moreover, along with the Exo III-assisted digestion reaction, target miRNA-182 was also released, which hybridized with unreacted Fc-H1 to trigger the next signal amplification reaction. Evidently, target miRNA-182 can initiate the 1:N amplified generation of Fc-mNs, as well as 1:N amplified lock of free MB molecules. Consequently, the opposite current changes of MB and Fc in the presence of miRNA-182 revealed that the proposed RHE strategy for target analyte sensitive biosensing is readily achieved.

Subsequently, DPV experiments of the sensing system under different conditions were carried out to validate the feasibility of the proposed RHE biosensor for miRNA-182 sensitive detection (Fig. 2A). The system comprising of Fc-H1, H2, H3, and MB displayed a high current of MB (I_{MB}) of 301 nA and a low current of Fc (I_{Fc}) of 23 nA, respectively (curve a), and the I_{Fc}/I_{MB} was calculated to be 0.076, impressively arguing the low degree of spontaneous interactions between Fc-H1, H2 and H3 in the absence of target miRNA-182. Further, the addition of Exo III made little influence on the I_{Fc}/I_{MB} value (curve b), which is consistent with the fact that Exo III can not change the structures of the DNA probes due to their single-stranded overhang 3'-termini. However, when target miRNA-182 was further added into the system, the oxidation current of Fc elevated to 225 nA, accompanied with that of MB decreased to 90 nA, which facilitate the I_{Fc}/I_{MB} value to increase to 2.50. Changing

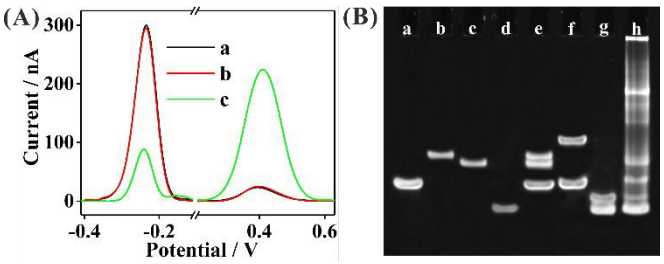

Fig. 2 (A) The DPV curves of the proposed sensing system under varied conditions: (a) Fc-H1 + H2 + H3 + MB; (b) Fc-H1 + H2 + H3 + MB + Exo III; (c) Fc-H1 + H2 + H3 + MB + miRNA-182 + Exo III. Experiments condition: [MB] = 3.0 μM; [Fc-H1] = 1.0 μM; [H2] = 1.0 μM; [H3] = 1.0 μM; [miRNA-182] = 10 pM. (B) Polyacrylamide gel electrophoresis (PAGE) confirmation of the working mechanism of the proposed sensing system under varied conditions. (a) H1; (b) H2; (c) H3; (d) miRNA-182; (e) H1 + H2 + H3 + Exo III; (f) H1 + miRNA-182; (g) H1 + miRNA-182 + Exo III; (h) H1 + H2 + H3 + miRNA-182 + Exo III.

Fc-H1 into Fc-H1′ or Fc-H1″ or Fc-H1‴, the proposed system displayed the I_{Fc}/I_{MB} value of 0.15 or 0.12 or 0.10 in the presence of miRNA-182, which is similar to that of the sensor developed by Fc-H1 in the absence of miRNA-182 and is much less than that in the presence of miRNA-182. Obviously, using the proposed strategy, RHE detection of miRNA can be readily realized based on the variation of I_{Fc}/I_{MB} value.

Further, gel electrophoresis experiment was applied to verify the hybridization recognition of Fc-H1 by target miRNA-182 and successful digestion of Fc-H1 in Fc-H1@182 complex by Exo III, as well as the generation of long duplex DNA chain originating from the HCR of H2 and H3. H1 has the same sequences with Fc-H1 and thus replaces Fc-H1 to avoid the interference of Fc in the experiment. It was worthy noting that mixing H1, H2, and H3 together does not lead to new band appearance (lane e), which is consistent with the DPV experimental results. When both H1 and miRNA-182 co-existed, a new band appeared in the behind of H1 attributable to the complex H1@182, accompanied with that of miRNA-182 disappeared (lane f), justifying the specific recognition of H1 by miRNA-182. Upon the addition of Exo III, the bands of H1@182 complex and H1 vanished, accompanied with that of miRNA-182 reappeared (lane g), implying that H1 in complex was digested and miRNA-182 was released to initiate Exo III-mediated cycling amplification reactions. In addition, it should be noted that a new band appeared in the behind of miRNA-182, corresponding well to the digestion product DNA trigger s1, which can activate the HCR of H2 and H3 to generate long duplex chain. As a consequence, lane h in Fig. 2B displayed newly appeared and consecutive bands at the lowest distance, corresponding well to the HCR products.

As a consequence of the aforementioned experimental results, we conclude that the proposed RHE biosensor can be used as a powerful candidate for accurate and sensitive detection of miRNA-182, and subsequently we evaluate its sensing performance through measuring the I_{Fc}/I_{MB} value of the sensing system subject to miRNA-182 with different amounts under the optimal conditions (Fig. S3, MB concentration 3.0 μM, Fc-H1 concentration 1.0 μM; Fig. S4, H2 concentration 1.0 μM, H3 concentration 1.0 μM; Fig. S5, reaction time 120 min). Fig. 3A depicts the DPV spectra recorded in the presence of miRNA-182 at different amounts. In comparison with control sample (in the absence of miRNA-182), the system displayed a gradually increased I_{Fc} and a gradually decreased I_{MB} along with the increased miRNA-182, corresponding well to the working mechanism that more miRNA-182 cause the generation of more Fc-mNs and the intercalation of more MB molecules in HCR products, thus varying their diffusion behavior and current responses. To quantitatively assess the performance of the proposed RHE biosensor for miRNA-182 assay, the working curve was drafted using I_{Fc}/I_{MB} value as vertical coordinate and miRNA-182 concentration ($C_{miRNA-182}$) as the horizontal coordinate (Fig. 3B). Evidently, the I_{Fc}/I_{MB} value is positively correlative with the increased miRNA-182 amount. Further, the I_{Fc}/I_{MB} was found to be linearly corresponding to logarithmic of $C_{miRNA-182}$ in the range from 0.01 to 10 pM, with a correlation equation of I_{Fc}/I_{MB} = -0.8263 + 0.7979log$C_{miRNA-182}$, and a coefficient of determination of R^2 = 0.9937 (Fig. 3C). It should be pointed out the as-proposed RHE strategy enjoyed exceptional analytical performance with a direct detection limit of 0.01 pM, which is not only comparable to that of previously reported electrochemical assays (Table S2), but also can effectively avoid the complicated procedures associated with electrode modification or material preparation. This exceptional performance may be attributable to the Exo III-assisted digestion cycling amplification and digestion product-initiated HCR, as well as the unique diffusion and intercalation behavior of Fc/MB, permitting for a rise in the number of Fc-mNs generated and an increase in the number of MB molecules

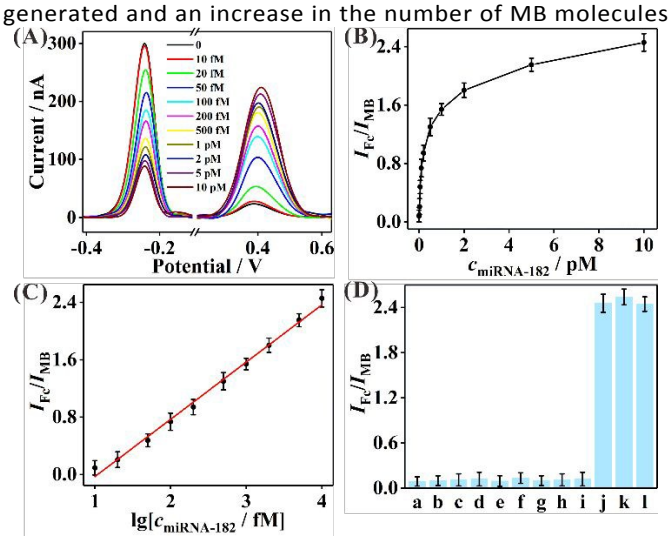

Fig. 3 (A) The DPV curves of the proposed RHE biosensor corresponding to miRNA-182 with different concentrations. (B) I_{Fc}/I_{MB} values vs the concentration of miRNA-182. (C) The linear relationship between the I_{Fc}/I_{MB} values and the logarithm of miRNA-182 concentration. Experiments condition: [MB] = 3.0 μM; [Fc-H1] = 1.0 μM; [H2] = 1.0 μM; [H3] = 1.0 μM; [miRNA-182] = 10 pM; [Reaction time] = 120 min. (D) Specific study of the proposed RHE biosensor. (a) control sample; (b) miRNA-21; (c) miRNA-96; (d) miRNA-382; (e) miRNA-183; (f) L-serine; (g) taurine; (h) ALT; (i) glucose; (j) miRNA-182; (k) miRNA-182 + miRNA-21 + miRNA-96 + miRNA-382 + miRNA-183; (l) miRNA-182 + L-serine + taurine + ALT + glucose. The concentrations of all interferences are 10 pM. The concentration of ALT was 20 U/L.

intercalated in the presence of a very small contribution of miRNA-182.

Besides sensitivity, specificity was investigated through using miRNA-21, miRNA-96, miRNA-382, miRNA-183, L-serine, taurine, alanine aminotransferase (ALT) and glucose as the interfering substances. The b, c, d, e, f, g, h, and i in Fig. 3D presented slight change in I_{Fc}/I_{MB} value compared with that of a in the absence of any target analyte, implying that these interfering substances could not switch on the Exo III-assisted cycling amplification reaction and subsequently influence the diagnosis results. Only when miRNA-182 existed, the sensing system depicted a significant rise in I_{Fc}/I_{MB} value. Moreover, a 10 pM miRNA-182 sample comprising of interfering substances manifested negligible I_{Fc}/I_{MB} value variation compared with that observed for 10 pM miRNA-182 alone. These evidences firmly validated the selectivity of the proposed RHE biosensor for discriminating target miRNA-182 from other miRNA members.

Achieving practical application in biological liquids is a great challenge for the proposed RHE biosensor, and thus serum obtained from glioma patients was employed as real sample to confirm this ability. It can be clearly seen from Fig. S6 that the serum sample displayed a relatively high I_{Fc}/I_{MB} value (1.01) compared with that of control sample (0.076). Based on the measured I_{Fc}/I_{MB} value, the miRNA-182 concentration in serum of glioma patients was calculated to be 2.01 pM using our method, which is in good agreement with the values determined from previously reported methods[25-27] and qRT-PCR method (2.08 pM). This above information justified the accuracy and reliability of the proposed RHE biosensor to sensitively detect miRNA in biological matrix.

In summary, a potential-resolved dual-signal homogeneous electrochemical strategy was proposed for ratiometric detection of target miRNA based on the target-initiated signal amplification reaction, in which Fc labeled ssDNA and free MB molecules were used as the electroactive probes. The experimental results demonstrated that diffusion between electroactive dyes and ITO electrode was greatly influenced by their existing forms, which provided a path to developing ratiometric homogeneous electrochemical biosensor without the involvement of complex electrode modification or material preparation. By making the best of Exo III-assisted target cycling and digestion product-activated HCR, more Fc-mNs were released into the system, accompanied with that more MB molecules were locked in HCR products, thus affording an increased I_{Fc}/I_{MB} value. Thus, exceptional miRNA sensing with high sensitivity and good selectivity was readily realized on the account of I_{Fc}/I_{MB} value change. More importantly, it exhibited fantastic accuracy and reliability for target miRNA detection in diluted serum obtained from glioma patients. Furthermore, this work revealed that such proposed strategy may be more suitable for future development of novel ratiometric homogeneous electrochemical biosensor because of the occurrence of all reactions in the same solution and no involvement of electrode modification/material preparation. Thus, this study was expected to provide a new thinking way for development of ratiometric homogeneous electrochemical biosensors for miRNA-related diseases diagnosis.

This work was financially supported by National Natural Science Foundation of China (21605093 and 21775082), and the Special Foundation for Distinguished Taishan Scholar of Shandong Province (ts201511052).

Notes and references

1 Y. Du, B. J. Lim, B. L. Li, Y. S. Jiang, J. L. Sessler and A. D. Ellington, *Anal. Chem.*, 2014, **86**, 8010–8016.
2 W. J. Shen, Y. Zhuo, Y. Q. Chai and R. Yuan, *Anal. Chem.*, 2015, **87**, 11345–11352.
3 A. Shamirian, H. S. Afsari, A. Hassan, L. W. Miller and P. T. Snee, *ACS Sensors*, 2016, **1**, 1244–1250.
4 R. Kawagoe, I. Takashima, S. Uchinomiya and A. Ojida, *Chem. Sci.*, 2017, **8**, 1134–1140.
5 A. T. Aron, M. O. Loehr, J. Bogena and C. J. Chang, *J. Am. Chem. Soc.*, 2016, **138**, 14338–14346.
6 S. Rana, S. G. Elci, R. Mout, A. K. Singla, M. Yazdani, M. Bender, A. Bajaj, K. Saha, U. H. Bunz, F. R. Jirik and V. M. Rotello, *J. Am. Chem. Soc.*, 2016, **138**, 4522–4529.
7 D. S. Richardson, C. Gregor, F. R. Winter, N. T. Urban, S. J. Sahl, K. I. Willig and S. W. Hell, *Nat. Commun.*, 2017, **8**, 577.
8 P. S. Zhang, H. Wang, Y. X. Hong, M. L. Yu, R. J. Zeng, Y. F. Long and J. Chen, *Biosens. Bioelectron.*, 2018, **99**, 318–324.
9 H. Y. Li, J. F. Chang, P. P. Gai and F. Li, *ACS Appl. Mater. Interfaces*, 2018, **10**, 4561–4568.
10 L. Ge, X. M. Sun, Q. Hong and F. Li, *ACS Appl. Mater. Interfaces*, 2017, **9**, 13102–13110.
11 C. Y. Deng, X. M. Pi, P. Qian, X. Q. Chen, W. M. Wu and J. Xiang, *Anal. Chem.*, 2017, **89**, 966–973.
12 X. B. Feng, N. Gan, H. R. Zhang, T. H. Li, Y. T. Cao, F. T. Hu and Q. L. Jiang, *Biosens. Bioelectron.*, 2016, **75**, 308–314.
13 S. Goggins, C. Naz, B. J. Marsh and C. G. Frost, *Chem. Commun.*, 2015, **51**, 561–564.
14 C. X. Zhu, M. Y. Liu, X. Y. Li, X. H. Zhang and J. H. Chen, *Chem. Commun.*, 2018, **54**, 10359–10362.
15 E. Xiong, Z. Z. Li, X. H. Zhang, J. W. Zhou, X. X. Yan, Y. Q. Liu and J. H. Chen, *Anal. Chem.*, 2017, **89**, 8830–8835.
16 W. Liu, H. Dong, L. M. Zhang and Y. Tian, *Angew. Chem. Int. Ed.*, 2017, **56**, 16328–16332.
17 X. P. Liu, Z. Q. Yan, Y. H. Sun, J. S. Ren and X. G. Qu, *Chem. Commun.*, 2017, **53**, 6215–6218.
18 L. L. Wang, R. N. Ma, L. S. Jiang, L. P. Jia, W. L. Jia and H. S. Wang, *Biosens. Bioelectron.*, 2017, **92**, 390–395.
19 J. F. Chang, X. Wang, J. Wang, H. Y. Li and F. Li, *Anal. Chem.*, 2019, **91**, 3604–3610.
20 T. Hou, W. Li, X. J. Liu and F. Li, *Anal. Chem.*, 2015, **87**, 11368–11374.
21 L. Ge, W. X. Wang and F. Li, *Anal. Chem.*, 2017, **89**, 11560–11567.
22 P. P. Gai, C. C. Gu, H. Y. Li, X. Z. Sun and F. Li, *Anal. Chem.*, 2017, **89**, 12293–12298.
23 E. Farjami, L. Clima, K. V. Gothelf and E. E. Ferapontova, *The Analyst*, 2010, **135**, 1443–1448.
24 F.-T. Zhang, J. Nie, D.-W. Zhang, J.-T. Chen, Y.-L. Zhou and X.-X. Zhang, *Anal. Chem.*, 2014, **86**, 9489–9495.
25 J. X. Wang, X. Y. Yi, H. L. Tang, H. X. Han, M. H. Wu and F. M. Zhou, *Anal. Chem.*, 2012, **84**, 6400–6406.
26 Z. X. Lu, H. L. Tang, D. H. Wu, Y. H. Xia, M. H. Wu, X. Y. Yi, H. F. Li and J. X. Wang, *Biosens. Bioelectron.*, 2016, **86**, 502–507.
27 J. R. Wang, Z. X. Lu, H. L. Tang, L. Wu, Z. X. Wang, M. H. Wu, X. Y. Yi and J. X. Wang, *Anal. Chem.*, 2017, **89**, 10834–10840.

